

TECHNICAL RESEARCH REPORT

A Dynamic Model for Magnetostrictive Hysteresis

by Xiaobo Tan, John S. Baras and P. S. Krishnaprasad

CDCSS TR 2002-6
(ISR TR 2002-41)



The Center for Dynamics and Control of Smart Structures (CDCSS) is a joint Harvard University, Boston University, University of Maryland center, supported by the Army Research Office under the ODDR&E MURI97 Program Grant No. DAAG55-97-1-0114 (through Harvard University). This document is a technical report in the CDCSS series originating at the University of Maryland.

Web site <http://www.isr.umd.edu/CDCSS/cdcss.html>

A Dynamic Model for Magnetostrictive Hysteresis*

Xiaobo Tan, John S. Baras and P. S. Krishnaprasad
 Institute for Systems Research and
 Department of Electrical and Computer Engineering
 University of Maryland, College Park, MD 20742 USA
 {xbtan, baras, krishna}@isr.umd.edu

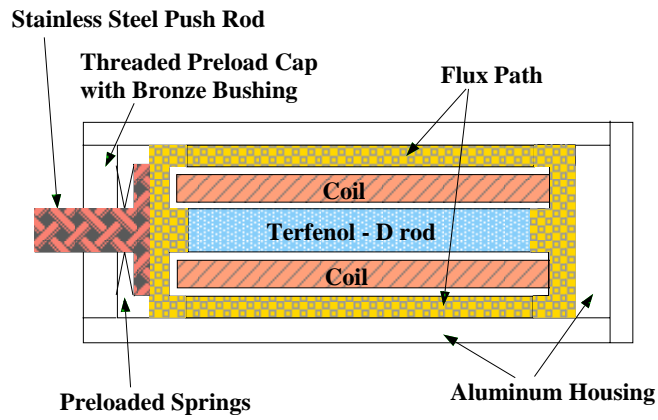
Abstract

The rate-dependent hysteresis present in thin magnetostrictive actuators can be captured by a dynamic model, consisting of a Preisach operator coupled to an ordinary differential equation in an unusual way. The model presents interesting problems in analysis and computation due to its special structure. In this paper we first transform the model into a more amenable form and gain insight into the model by introducing a new hysteretic operator. Then we investigate some system-theoretic properties of the model: stability of equilibria, input-output stability, reachability and controllability. Existence of periodic solutions under periodic forcing is also established. Finally numerical integration schemes for the model are discussed.

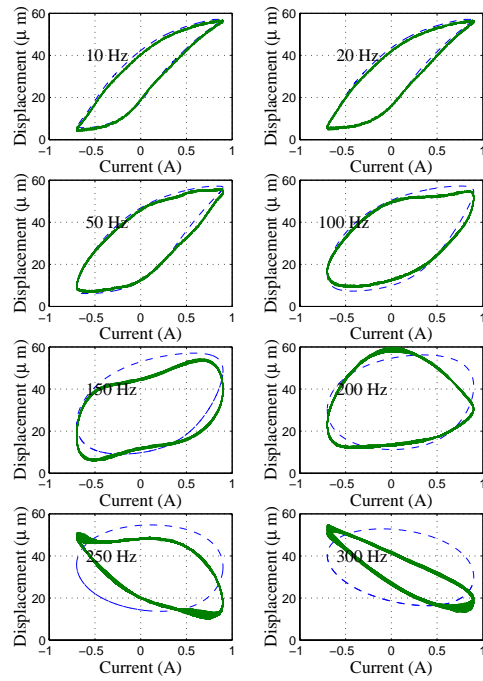
1 Introduction

Magnetostriction is the phenomenon of strong coupling between magnetic properties and mechanical properties of some ferromagnetic materials (e.g., Terfenol-D): strains are generated in response to an applied magnetic field, while conversely, mechanical stresses in the materials produce measurable changes in magnetization. This phenomenon can be used for actuation and sensing. Magnetostrictive actuators have applications in micro-positioning, robotics, ultrasonics, vibration control, etc. Figure 1(a) shows a sectional view of a Terfenol-D actuator manufactured by Etrema Products, Inc. By varying the current in the coil, we vary the magnetic field in the Terfenol-D rod and thus control the motion of the rod head.

*This research was supported by the Army Research Office under the ODDR&E MURI97 Program Grant No. DAAG55-97-1-0114 to the Center for Dynamics and Control of Smart Structures (through Harvard University).



(a)



(b)

Figure 1: (a) Sectional view of a Terfenol-D actuator [1](Original source: Etrema Products, Inc.). (b) The rate-dependent magnetostrictive hysteresis. Solid line: experimental measurement; Dashed line: numerical prediction based on the dynamic model [2].

Like any other smart material, magnetostrictive materials exhibit hysteresis, which hinders their wider applicability in actuators and sensors. A fundamental idea in coping with hysteresis is to formulate the mathematical model of hysteresis and use inverse compensation to cancel out the hysteretic effect. There have been a few monographs devoted to modeling of hysteresis and study of dynamical systems with hysteresis [3, 4, 5, 6]. Hysteresis models can be roughly classified into physics-based models, see e.g., [7, 8, 9], and phenomenological models. The most popular phenomenological hysteresis model used in control of smart actuators has been the Preisach model [10, 11, 12, 13]. Although in general the Preisach model does not provide physical insight into the problem, it provides a means of developing phenomenological models that are capable of producing behaviors similar to those of physical systems.

The hysteretic behavior of a magnetostrictive actuator at low frequencies (typically below 5 Hz) is rate-independent: roughly speaking, the shape of the hysteresis loop does not depend on the frequency of the input. This is no longer the case when the operating frequency gets high, due to the eddy current effect and the magnetoelastic dynamics of the magnetostrictive rod (Figure 1(b)). The (rate-independent) Preisach operator alone is not capable of modeling the rate-dependent hysteresis. A novel dynamic model for the magnetostrictive hysteresis has been proposed in [14, 2], and it can capture the high frequency effects in magnetostrictive actuators (see the comparison in Figure 1(b)). In the model, a Preisach operator is coupled to an ordinary differential equation (ODE) in an unusual way. Based on the model one can develop efficient inverse control and robust control algorithms which are implementable in real-time [14]. Apart from being useful for the control purpose, the model presents interesting problems in analysis and computation due to its special structure.

The remainder of the paper is organized as follows. Section 2 provides an introduction to the Preisach operator. In Section 3 we describe the model and provide a new perspective to study the model. Some system-theoretic properties of the model are investigated in Section 4. Existence of periodic solutions under periodic forcing is established in Section 5. We discuss numerical integration schemes for the model in Section 6. Concluding remarks are provided in Section 7.

2 The Preisach Model

For a pair of thresholds (β, α) with $\beta \leq \alpha$, consider a simple hysteretic element $\hat{\gamma}_{\beta, \alpha}[\cdot, \cdot]$, as illustrated in Figure 2. For $u \in C([0, T])$ and an initial configuration $\zeta \in \{-1, 1\}$, the function $v = \hat{\gamma}_{\beta, \alpha}[u, \zeta] : [0, T] \rightarrow$

$\{-1, 1\}$ is defined as follows [5]:

$$v(0) \triangleq \begin{cases} -1 & \text{if } u(0) \leq \beta \\ \zeta & \text{if } \beta < u(0) < \alpha \\ 1 & \text{if } u(0) \geq \alpha \end{cases},$$

and for $t \in (0, T]$, setting $X_t \triangleq \{\tau \in (0, t] : u(\tau) = \beta \text{ or } \alpha\}$,

$$v(t) \triangleq \begin{cases} v(0) & \text{if } X_t = \emptyset \\ -1 & \text{if } X_t \neq \emptyset \text{ and } u(\max X_t) = \beta \\ 1 & \text{if } X_t \neq \emptyset \text{ and } u(\max X_t) = \alpha \end{cases}.$$

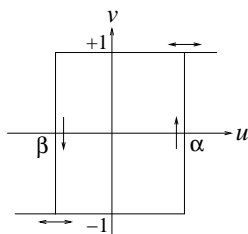


Figure 2: The elementary Preisach hysteron.

This operator is sometimes referred to as an *elementary Preisach hysteron* (we will call it a *hysteron* in this paper), since it is a building block for the Preisach operator.

The Preisach operator is a weighted superposition of all possible hysterons. Define $\mathcal{P}_0 \triangleq \{(\beta, \alpha) \in \mathbb{R}^2 : \beta \leq \alpha\}$. \mathcal{P}_0 is called the *Preisach plane*, and each $(\beta, \alpha) \in \mathcal{P}_0$ is identified with the hysteron $\hat{\gamma}_{\beta, \alpha}$. For $u \in C([0, T])$ and a Borel measurable initial configuration ζ_0 of all hysterons: $\zeta_0 : \mathcal{P}_0 \rightarrow \{-1, 1\}$, the output of the Preisach operator Γ is defined as [5]:

$$y(t) = \Gamma[u, \zeta_0](t) = \int_{\mathcal{P}_0} \hat{\gamma}_{\beta, \alpha}[u, \zeta_0(\beta, \alpha)](t) d\nu(\beta, \alpha), \quad (1)$$

where ν is a finite, signed Borel measure on \mathcal{P}_0 , called the *Preisach measure*.

We call the Preisach measure ν *nonsingular* if $|\nu|$ is absolutely continuous with respect to the two-dimensional Lebesgue measure, and *singular* otherwise. By the Radon-Nikodym theorem [15], if ν is nonsingular, there exists a Borel measurable function μ , such that

$$\Gamma[u, \zeta_0](t) = \int \int_{\mathcal{P}_0} \mu(\beta, \alpha) \hat{\gamma}_{\beta, \alpha}[u, \zeta_0(\beta, \alpha)](t) d\beta d\alpha. \quad (2)$$

The weighting function μ is often referred to as the *Preisach function* [4] or the *density function* [6].

To simplify the discussion, throughout the paper we assume that μ has a compact support, i.e., $\mu(\beta, \alpha) = 0$ if $\beta < \beta_0$ or $\alpha > \alpha_0$ for some β_0, α_0 , and without loss of generality, we let $\alpha_0 = -\beta_0 =: r_0 > 0$. Then it suffices to consider the finite triangular area $\mathcal{P} \triangleq \{(\beta, \alpha) \in \mathbb{R}^2 \mid \alpha \geq \beta, \beta \geq -r_0, \alpha \leq r_0\}$.

At time t , \mathcal{P} can be divided into two regions: $\mathcal{P}_\pm(t) \triangleq \{(\beta, \alpha) \in \mathcal{P} \mid \text{output of } \hat{\gamma}_{\beta, \alpha} \text{ at } t \text{ is } \pm 1\}$. In most cases of interest, each of \mathcal{P}_- and \mathcal{P}_+ is a connected set [4], and the output of Γ is determined by the boundary between \mathcal{P}_- and \mathcal{P}_+ if the Preisach measure is nonsingular. The boundary is also called the *memory curve*. The memory curve has a staircase structure and its intersection with the line $\alpha = \beta$ gives the current input value. The memory curve ψ_0 at $t = 0$ is called the *initial memory curve* and it represents the initial condition of the Preisach operator.

If the Preisach measure is nonsingular, we can identify a configuration of hysterons ζ_ψ with a memory curve ψ in the following way: $\zeta_\psi(\beta, \alpha) = 1$ (-1 , resp.) if (β, α) is below (above, resp.) the graph of ψ . Note that it does not matter whether ζ_ψ takes 1 or -1 on the graph of ψ . In the sequel we will put the initial memory curve ψ_0 as the second argument of Γ , where $\Gamma[\cdot, \psi_0] \triangleq \Gamma[\cdot, \zeta_{\psi_0}]$.

Sometimes it is more convenient to describe the Preisach operator using the (r, s) coordinates with $r = \frac{\alpha - \beta}{2}$ and $s = \frac{\alpha + \beta}{2}$. In the new coordinates, a memory curve ψ is the graph of a function of r , and $\psi(0)$ gives the current input value. Although practically a memory curve is only composed of segments of slope ± 1 in (r, s) coordinates, we make the following definition to facilitate the analysis [6, 16]:

Definition 2.1 *The set of memory curves Ψ is defined to be the set of continuous functions $\psi : [0, r_0] \rightarrow \mathbb{R}$ such that*

1. $|\psi(r_1) - \psi(r_2)| \leq |r_1 - r_2|, \forall r_1, r_2 \in [0, r_0];$
2. $\psi(r_0) = 0.$

We will switch between the (β, α) coordinates and the (r, s) coordinates in this paper.

Theorem 2.1 summarizes some basic properties of the Preisach operator, see, e.g., [5].

Theorem 2.1 [5]: *Let ν be a Preisach measure. Let $u, u_1, u_2 \in C([0, T])$ and $\psi_0 \in \Psi$. Then the*

following hold:

1. **(Rate Independence)** If $\phi : [0, T] \rightarrow [0, T]$ is an increasing continuous function satisfying $\phi(0) = 0$ and $\phi(T) = T$, then $\Gamma[u \circ \phi, \psi_0](t) = \Gamma[u, \psi_0](\phi(t))$, $\forall t \in [0, T]$, where “ \circ ” denotes composition of functions.
2. **(Strong Continuity)** If ν is nonsingular, then $\Gamma[\cdot, \psi_0] : C([0, T]) \rightarrow C([0, T])$ is strongly continuous (in the sup norm).
3. **(Piecewise Monotonicity)** Let $\nu \geq 0$. If u is either nondecreasing or nonincreasing on some interval in $[0, T]$, then so is $\Gamma[u, \psi_0]$.
4. **(Order Preservation)** Let $\nu \geq 0$. If $u_1 \leq u_2$ on $[0, T]$, then $\Gamma[u_1, \psi_0] \leq \Gamma[u_2, \psi_0]$ on $[0, T]$.

Theorem 2.2 (Lipschitz continuity) [6]¹ Assume that the Preisach measure ν is nonsingular. Let ω be the Preisach density function in (r, s) coordinates. Then for any $\psi_0 \in \Psi$, $\Gamma[\cdot, \psi_0]$ is Lipschitz continuous on $C([0, T])$ with Lipschitz constant $2C_1$ if

$$C_1 \triangleq \int_0^\infty \sup_{s \in \mathbb{R}} |\omega(r, s)| dr < \infty. \quad (3)$$

3 A Dynamic Model for the Hysteresis

Venkataraman and Krishnaprasad proposed a bulk magnetostrictive hysteresis model for the thin rod actuator based on energy balancing principles [17, 1]. The model has a cascaded structure as shown in Figure 3. \bar{W} takes care of the $M - H$ hysteresis and the eddy current losses, where M and H denote the bulk magnetization and the magnetic field (assumed uniform) along the rod direction, respectively. The magnetoelastic dynamics of the rod is lumped into a second order linear system $G(s)$. In [17, 1], the $M - H$ hysteresis was described by a low dimensional ferromagnetic hysteresis model and that leads to a switching ODE model for \bar{W} .

A new dynamic model for \bar{W} has been proposed in [14, 2], where the Preisach operator Γ is used to model the $M - H$ hysteresis:

$$\begin{cases} \dot{H}(t) + \dot{M}(t) = c_1(I(t) - \frac{H(t)}{c_0}) \\ M(t) = \Gamma[H(\cdot), \psi_0](t) \end{cases}, \quad (4)$$

¹See also [5] for a slightly different version.

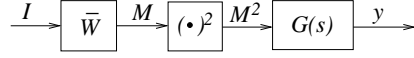


Figure 3: Model structure of a magnetostrictive actuator.

where I is the input current, $c_0 > 0$ and $c_1 > 0$ are constants.

Eq. (4) presents interesting problems in analysis due to its special structure. The well-posedness of (4) when the Preisach measure ν is nonnegative and nonsingular, was proved in [2] using the Euler polygon method. In this section we present another perspective for study of (4), which will provide an alternative proof of the well-posedness as well as new insight into understanding of (4).

We define an operator $\mathcal{B} : C([0, T]) \times \Psi \rightarrow C([0, T])$, such that for $H \in C([0, T])$, $\psi_0 \in \Psi$,

$$\mathcal{B}[H, \psi_0](t) = H(t) + \Gamma[H, \psi_0](t). \quad (5)$$

Let $\tilde{B} = \mathcal{B}[H, \psi_0]$. Note the physical interpretation of \tilde{B} is the scaled magnetic flux density. If $\mathcal{B}[\cdot, \psi_0]$ is invertible, Eq. (4) can be written as:

$$\dot{\tilde{B}}(t) = c_1(I(t) - \frac{\mathcal{B}^{-1}[\tilde{B}(\cdot), \psi_0](t)}{c_0}). \quad (6)$$

Eq. (6) is of a more amenable form and people have studied such systems, see [6] and the references therein.

For an interval J , we define $C_J([0, T]) \triangleq \{u \in C([0, T]) : u(t) \in J, \forall t \in [0, T]\}$. Let $J_H = [H_{min}, H_{max}] \subset \mathbb{R}$ be the range of H . Then $\Gamma : C_{J_H}([0, T]) \times \Psi \rightarrow C_{J_M}([0, T])$, where the interval $J_M = [M_{min}, M_{max}]$ and M_{min} (M_{max} , resp.) is the negative (positive, resp.) saturation corresponding to H_{min} (H_{max} , resp.). Let $J_B = [H_{min} + M_{min}, H_{max} + M_{max}]$.

Proposition 3.1 *Let the Preisach measure ν be nonnegative and nonsingular. Then $\forall \psi_0 \in \Psi$,*

$$\mathcal{B}[\cdot, \psi_0] : C_{J_H}([0, T]) \rightarrow C_{J_B}([0, T])$$

is rate-independent, strongly continuous, piecewise monotone, order preserving, and injective.

Proof. It's straightforward that the range of $\mathcal{B}[\cdot, \psi_0]$ is a subset of $C_{J_B}([0, T])$, and $\mathcal{B}[\cdot, \psi_0]$ is piecewise monotone and rate-independent. Continuity and order preservation of $\mathcal{B}[\cdot, \psi_0]$ follows from those of $\Gamma[\cdot, \psi_0]$. The injectivity can also be shown using the order preservation property of Γ . \square

The following lemma will be useful for proving the surjectivity of $\mathcal{B}[\cdot, \psi_0]$:

Lemma 3.1 [5]: *Let X, Y be metric spaces, $f : X \rightarrow Y$ be continuous and $\tilde{Y} \subset f(X)$ be dense in Y . Also assume that for any relatively compact set $K \subset \tilde{Y}$, the set $f^{-1}(K) \triangleq \{x \in X : f(x) \in K\}$ is relatively compact. Then $f(X) = Y$. If moreover f is injective, then $f^{-1} : Y \rightarrow X$ is continuous.*

For $u \in C([0, T])$, we define $\underset{[t_1, t_2]}{\text{osc}} u \triangleq \max_{[t_1, t_2]} u - \min_{[t_1, t_2]} u, \forall [t_1, t_2] \subset [0, T]$.

Lemma 3.2 *Let μ be nonsingular and nonnegative. Then $\forall \psi_0 \in \Psi, \forall H \in C([0, T])$,*

$$\underset{[t_1, t_2]}{\text{osc}} H \leq \underset{[t_1, t_2]}{\text{osc}} \mathcal{B}[H, \psi_0], \quad \forall [t_1, t_2] \subset [0, T]. \quad (7)$$

Proof. Let $t^* = \arg \max_{[t_1, t_2]} H, t_* = \arg \min_{[t_1, t_2]} H$. It's easy to verify that $\Gamma[H, \psi_0](t^*) \geq \Gamma[H, \psi_0](t_*)$.

Hence

$$\underset{[t_1, t_2]}{\text{osc}} \mathcal{B}[H, \psi_0] \geq \mathcal{B}[H, \psi_0](t^*) - \mathcal{B}[H, \psi_0](t_*) \geq \underset{[t_1, t_2]}{\text{osc}} H. \quad \square$$

Theorem 3.1 *Let the Preisach measure ν be nonnegative and nonsingular. Then for any $\psi_0 \in \Psi$, $\mathcal{B}[\cdot, \psi_0]$ is surjective, and its inverse $\mathcal{B}^{-1}[\cdot, \psi_0] : C_{J_B}([0, T]) \rightarrow C_{J_H}([0, T])$ is continuous.*

Proof. The results will follow from Lemma 3.1, by letting $X = C_{J_H}([0, T]), Y = C_{J_B}([0, T])$, $f = \mathcal{B}[\cdot, \psi_0]$, and $\tilde{Y} = C_{pm, J_B}([0, T]) \triangleq \{u \in C_{J_B}([0, T]) : u \text{ is piecewise monotone}\}$. We now verify that the assumptions in Lemma 3.1 are satisfied.

From Proposition 3.1, f is continuous and injective. \tilde{Y} is obviously dense in Y . Using a technique in [18], one can show $\tilde{Y} \subset f(X)$. We are left to show $f^{-1}(K)$ is relatively compact for any relatively compact set $K \subset \tilde{Y}$. Using Lemma 3.2, the set $\mathcal{B}^{-1}[K, \psi_0]$ is equicontinuous if $K \subset C_{pm, J_B}([0, T])$ is. Then we conclude with the Ascoli-Arzelá Theorem. \square

It turns out that a stronger result holds:

Theorem 3.2 *Let the Preisach measure ν be nonnegative and nonsingular. Then $\forall \psi_0 \in \Psi, \mathcal{B}^{-1}[\cdot, \psi_0]$ is Lipschitz continuous with Lipschitz constant 2.*

Theorem 3.2 can be shown by adapting the proof of Lipschitz continuity of Γ^{-1} in [19] when some additional conditions on ν are satisfied, see [14]. Using Theorem 3.2, one can easily show the existence and uniqueness of the solution to (6), see Theorem 3.1.1 in [6].

We can also show that \mathcal{B}^{-1} is Lipschitz continuous with respect to both arguments, from which we can obtain an explicit formula for continuous dependence of the solution to (4) on initial conditions [14].

4 System-Theoretic Properties of the Model

In this section, we study system-theoretic properties associated with the infinite dimensional hysteretic system (4). In particular, we look at stability of equilibria, input-output stability, reachability and observability.

4.1 Stability of equilibria

The state for (4) is the (infinite-dimensional) memory curve $\psi \in \Psi$ since both H and M can be derived from ψ . We set the input $I \equiv 0$ in (4) and investigate stability of the equilibria of the following equation:

$$\begin{cases} \dot{H}(t) + \dot{M}(t) = -\frac{c_1}{c_0}H(t) \\ M(t) = \Gamma[H(\cdot), \psi_0](t) \end{cases} \quad (8)$$

We can easily see that in (r, s) coordinates, the set of equilibria is $\Psi_0 = \{\psi \in \Psi : \psi(0) = 0\}$.

Recall the definition of ζ_ψ for $\psi \in \Psi$ in Section 2. For $\psi_1, \psi_2 \in \Psi$, we define

$$\|\psi_1 - \psi_2\| \stackrel{\Delta}{=} \int \int_P |\zeta_{\psi_1}(\beta, \alpha) - \zeta_{\psi_2}(\beta, \alpha)| d\beta d\alpha. \quad (9)$$

If the Preisach density μ is continuous, for $\psi \in \Psi$, we can define $\frac{dM}{dH}(\psi, +)$ ($\frac{dM}{dH}(\psi, -)$, resp.), which carries the interpretation of the derivative of M with respect to H when H is being increased (decreased, resp.) at the state ψ [14]. Furthermore, if $\mu \geq 0$, we have

$$0 \leq \frac{dM}{dH}(\psi, \pm) \leq C, \quad (10)$$

for some $C > 0$.

Proposition 4.1 *Assume that the Preisach measure is nonnegative, and nonsingular with a piecewise continuous density μ . Then every $\psi \in \Psi_0$ is a stable but not asymptotically stable equilibrium of (8).*

Proof. Consider $\psi^* \in \Psi_0$. Denote $\psi[t]$ the memory curve at t when the system starts from $\psi_0 \in \Psi$ at $t = 0$. For a.e. t , the first equation in (8) can be rewritten as $\dot{H}(t) = -\frac{c_1 H(t)}{c_0(1 + \frac{dM}{dH}(\psi[t], \text{sgn}(\dot{H}(t))))}$, which implies $H(t) \rightarrow 0$ asymptotically. Therefore $\|\psi[t] - \psi^*\| \leq \|\psi_0 - \psi^*\|$, $\forall t \geq 0$, and ψ^* is stable. ψ^* is not asymptotically stable since Ψ_0 forms a continuum. \square

Remark 4.1 *Although any individual $\psi \in \Psi_0$ is not asymptotically stable, Ψ_0 is “globally asymptotically stable”, in the sense that, starting from any $\psi_0 \in \Psi$, $\lim_{t \rightarrow \infty} \inf_{\psi \in \Psi_0} \|\psi[t] - \psi\| = 0$.*

4.2 Input-output stability

For each $\psi_0 \in \Psi$, the system (4) defines a mapping from the input $I(\cdot)$ to the output $\{H(\cdot), M(\cdot)\}$. Here we focus on the finite gain L_2 stability and the finite gain L_∞ stability [20] from $I(\cdot)$ to $H(\cdot)$ since the case from $I(\cdot)$ to $M(\cdot)$ is not as interesting [21].

Proposition 4.2 *Let the Preisach measure be nonnegative and nonsingular. Then $\forall \psi_0 \in \Psi$, for any piecewise continuous $I(\cdot)$ with finite L_∞ norm,*

$$\|H(\cdot)\|_\infty \leq \max\{|H(0)|, c_0 \|I(\cdot)\|_\infty\}. \quad (11)$$

Proof. Due to the piecewise monotonicity of Γ ,

$$\dot{H} \geq 0 \text{ if } I(t) \geq \frac{H(t)}{c_0}, \text{ and } \dot{H} \leq 0 \text{ if } I(t) \leq \frac{H(t)}{c_0}$$

which lead to the result. \square

Proposition 4.3 *Let the Preisach measure be nonnegative and nonsingular with a piecewise continuous density μ . Then $\forall \psi_0 \in \Psi$, for any piecewise continuous $I(\cdot)$ with finite L_2 norm,*

$$\|H(\cdot)\|_2 \leq \bar{\gamma} \|I(\cdot)\|_2 + \bar{b}_0, \quad (12)$$

where $\bar{\gamma} = \sup_\omega \frac{c_1}{|j\omega + \frac{c_1}{c_0(1+C)}|}$, $\bar{b}_0 = \sqrt{\frac{c_0(1+C)}{2c_1}} |H(0)|$, and C is the constant in (10).

Sketch of proof. Rewrite (4) as $\dot{H}(t) = -\frac{c_1}{c_0(1+g(t))} H(t) + \frac{c_1}{1+g(t)} I(t)$, where $g(t) = \frac{dM}{dH}(\psi[t], \text{sgn}(\dot{H}(t)))$. Then (12) can be derived using the bounds on $g(t)$ and the Parseval's identity [14]. \square

4.3 Reachability and observability

Let $\psi[t]$ denote the memory curve at time t . For any $I(\cdot) \in PC([0, T])$ (the space of piecewise continuous functions), the corresponding $\psi[\cdot]$ is continuous in the metric (9) and we write $\psi[\cdot] \in C([0, T], \Psi)$. Denote $\Xi : PC([0, T]) \times \Psi \rightarrow C([0, T], \Psi)$ the state evolution map for (4), i.e., for $I(\cdot) \in PC([0, T])$ and $\psi[0] \in \Psi$, $\psi[t] = \Xi[I(\cdot), \psi[0]](t)$.

Definition 4.1 (Reachability and Approximate Reachability for (4)) *We say $\psi_2 \in \Psi$ is reachable from $\psi_1 \in \Psi$ if $\exists T < \infty$, and $I(\cdot) \in PC([0, T])$, such that $\psi_2 = \Xi[I(\cdot), \psi_1](T)$. We say $\psi_2 \in \Psi$ is approximately reachable from $\psi_1 \in \Psi$ if for any $\epsilon > 0$, $\exists \psi_\epsilon \in \Psi$ such that ψ_ϵ is reachable from ψ_1 and $\|\psi_\epsilon - \psi_2\| \leq \epsilon$. The state space Ψ is reachable (approximately reachable, resp.) if any state is reachable (approximately reachable, resp.) from any other state.*

Definition 4.2 (Observability for (4)) *We say $\psi_1 \in \Psi$ is distinguishable from $\psi_2 \in \Psi$, if $\exists T < \infty$ and $I(\cdot) \in PC([0, T])$, such that $H_1(t') \neq H_2(t')$ or $M_1(t') \neq M_2(t')$, for some $t' \in [0, T]$. The system (4) is observable if any state $\psi \in \Psi$ is distinguishable from any other state.*

The proofs for the following results are omitted due to space limitation and they can be found in [14].

Proposition 4.4 *Let the Preisach measure be nonnegative and nonsingular. The state space Ψ for (4) is not reachable, but approximately reachable.*

Proposition 4.5 *Let the Preisach measure be nonnegative and nonsingular with density μ . The system (4) is observable if and only if $\forall \psi_1, \psi_2 \in \Psi$ and $\psi_1 \neq \psi_2$, $\int \int_P \mu(\beta, \alpha) |\zeta_{\psi_1}(\beta, \alpha) - \zeta_{\psi_2}(\beta, \alpha)| d\beta d\alpha > 0$.*

5 Existence of Periodic Solutions

Theorem 5.1 *Let the Preisach measure be nonnegative and nonsingular. Define $J_I = [\frac{H_{min}}{c_0}, \frac{H_{max}}{c_0}]$. Let $I \in C_{J_I}([0, \infty))$ be T -periodic, i.e., $I(t+T) = I(t)$, $\forall t \geq 0$. Let $\Xi : C([0, \infty)) \times \Psi \rightarrow C([0, \infty), \Psi)$ be the state evolution map for (4). Then there exists $\psi_0 \in \Psi$, such that $\Xi[I, \psi_0](t+T) = \Xi[I, \psi_0](t)$, $\forall t \geq 0$.*

Proof. Denote $L_1([0, r_0])$ the Banach space of integrable functions on $[0, r_0]$. First we show Ψ is a closed subset of $L_1([0, r_0])$, where we borrow some ideas from the proof of Theorem 3.3 in [16].

In (r, s) coordinates, any $\psi \in \Psi$ is a continuous function of r on $[0, r_0]$, and thus $\psi \in L_1([0, r_0])$. Let a sequence $\{\psi_n \in \Psi\}$ converge to $\tilde{\psi} \in L_1([0, r_0])$ in the L_1 norm. By definition of Ψ , $\{\psi_n\}$ is equicontinuous and equibounded. Therefore by the Ascoli-Arzelá Theorem, a subsequence $\psi_{n_k} \rightarrow \bar{\psi} \in \Psi$ uniformly on $[0, r_0]$, which implies $\{\psi_{n_k}\}$ converges to $\bar{\psi}$ in L_1 . Therefore $\tilde{\psi} = \bar{\psi}$ and Ψ is closed.

Given $\psi_0 \in \Psi$ and a T -periodic $I \in C_{J_I}([0, \infty))$, we have $\Xi[I, \psi_0](t) \in \Psi, \forall t \geq 0$, from Proposition 4.2. We then define the map $\Xi_T : \Psi \rightarrow \Psi$ by

$$\Xi_T(\psi_0) \triangleq \Xi[I, \psi_0](T), \quad \forall \psi_0 \in \Psi. \quad (13)$$

It's easy to verify that Ξ_T is continuous. Also Ξ_T is a compact mapping since Ψ itself is compact. Finally Ψ is a convex set. Therefore Ξ_T has a fixed point by the Schauder fixed point theorem, and this completes the proof. \square

Remark 5.1 *Theorem 5.1 implies that the corresponding solution $\{H(\cdot), M(\cdot)\}$ is also periodic.*

Remark 5.2 *We observe a periodic motion of the actuator head when a periodic input is applied. Existence of periodic solutions to (4) under periodic forcing partially validates the model. This result also provides a theoretical basis for the parameter identification method in [2].*

6 Numerical Integration of the Model

Numerically solving (4) helps predict behaviors of the model, verify theoretical analysis, and validate the model by comparing the simulation result to the experimental measurement. Given the memory curve $\psi[t_0]$ at time t_0 and the input $I(\cdot)$, approximate values of H and M at $t_0 + h$ can be computed by an Euler method:

$$\begin{cases} \frac{\tilde{H}(t_0+h)-H(t_0)}{h} + \frac{\tilde{M}(t_0+h)-M(t_0)}{h} = c_1(I(t_0) - \frac{H(t_0)}{c_0}) \\ \tilde{M}(t_0 + h) = \Gamma[\tilde{H}(t_0 + h), \psi[t_0]] \end{cases}, \quad (14)$$

where h is the time step size. Eq. (14) can be solved by adapting the inversion schemes for Γ [14].

We have the following result about accuracy of the algorithm (14) and its proof can be found in [14]:

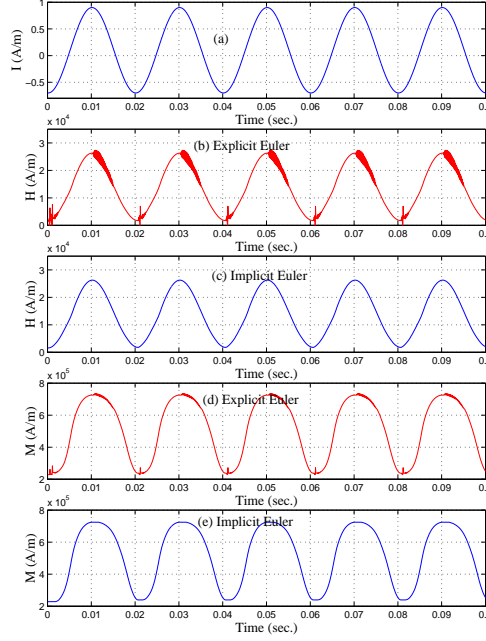


Figure 4: Comparison of the implicit Euler scheme with the explicit Euler scheme. $h = 8 \times 10^{-5}$ second. (a): the input current; (b), (d): trajectories of H , M computed by the explicit scheme; (c), (e): trajectories of H , M computed by the implicit scheme.

Proposition 6.1 *Assume that the Preisach measure is nonnegative, nonsingular with a piecewise continuous density μ . Assume the input $I(\cdot)$ is continuous and bounded. Consider the algorithm (14). Let the true solution to (4) be $\{H(\cdot), M(\cdot)\}$. Assume $\frac{dM}{dH}(\psi[t_0], \pm)$ and the derivatives of $H(t)$ and $M(t)$ at t_0 exist. Then*

$$|\tilde{H}(t_0 + h) - H(t_0 + h)| = \mathcal{O}(h^2), \quad (15)$$

$$|\tilde{M}(t_0 + h) - M(t_0 + h)| = \mathcal{O}(h^2). \quad (16)$$

We call (14) the *explicit Euler* scheme since $\tilde{H}(t_0 + h)$ is not involved in the right-hand side of the first equation in (14). We obtain the *implicit* scheme by replacing $I(t_0)$ and $H(t_0)$ in the right hand side of (14) with $I(t_0 + h)$ and $\tilde{H}(t_0 + h)$, respectively. We note that the implicit scheme requires no more computational effort than the explicit one, but it's much more stable and can provide meaningful solutions even when h is not very small (Figure 4).

7 Conclusions

This paper has been devoted to analysis of a rate-dependent hysteresis model. By introducing a new hysteretic operator \mathcal{B}^{-1} , we have transformed the model into a more familiar form and gained deeper insight into the model. Various system-theoretic properties have been examined for this infinite-dimensional hysteretic system. We have proved the existence of periodic solutions under periodic forcing. We have also presented numerical schemes for simulation of the model.

References

- [1] R. Venkataraman, *Modeling and Adaptive Control of Magnetostrictive Actuators*, Ph.D. thesis, University of Maryland, College Park, 1999.
- [2] X. Tan and J. S. Baras, “Modeling and control of a magnetostrictive actuator,” in *the Proceedings of the 41st IEEE Conference on Decision and Control (to appear)*, Las Vegas, NV, 2002.
- [3] M. A. Krasnosel’skii and A. V. Pokrovskii, *Systems with Hysteresis*, Springer-Verlag, 1989.
- [4] I. D. Mayergoyz, *Mathematical Models of Hysteresis*, Springer Verlag, 1991.
- [5] A. Visintin, *Differential Models of Hysteresis*, Springer, 1994.
- [6] M. Brokate and J. Sprekels, *Hysteresis and Phase Transitions*, Springer Verlag, New York, 1996.
- [7] D. C. Jiles and D. L. Atherton, “Theory of ferromagnetic hysteresis,” *Journal of Magnetism and Magnetic Materials*, vol. 61, pp. 48–60, 1986.
- [8] R. Venkataraman and P. S. Krishnaprasad, “Qualitative analysis of a bulk ferromagnetic hysteresis model,” in *Proceedings of the 37th IEEE Conference on Decision and Control, Tampa, FL, Dec. 1998*, pp. 2443–2448.
- [9] M. J. Dapino, *Nonlinear and Hysteretic Magnetomechanical Model for Magnetostrictive Transducers*, Ph.D. thesis, Iowa State University, Ames, Iowa, 1999.
- [10] D. Hughes and J. T. Wen, “Preisach modeling and compensation for smart material hysteresis,” in *Active Materials and Smart Structures*, G. L. Anderson and D. C. Lagoudas, Eds., 1994, vol. 2427 of *SPIE*, pp. 50–64.

- [11] P. Ge and M. Jouaneh, "Tracking control of a piezoceramic actuator," *IEEE Transactions on Control Systems Technology*, vol. 4, no. 3, pp. 209–216, 1996.
- [12] R. B. Gorbet, D. W. L. Wang, and K. A. Morris, "Preisach model identification of a two-wire SMA actuator," in *Proceedings of IEEE International Conference on Robotics and Automation*, 1998, pp. 2161–2167.
- [13] X. Tan, R. Venkataraman, and P. S. Krishnaprasad, "Control of hysteresis: Theory and experimental results," in *Modeling, Signal Processing, and Control in Smart Structures*, V. S. Rao, Ed., 2001, vol. 4326 of *SPIE*, pp. 101–112.
- [14] X. Tan, *Control of Smart Actuators*, Ph.D. thesis, University of Maryland, College Park, MD, Sept. 2002, available online at <http://www.isr.umd.edu/TechReports/ISR/2002>, in the PhD Thesis section.
- [15] H. L. Royden, *Real Analysis*, Prentice Hall, Englewood Cliffs, NJ, 1988.
- [16] R. B. Gorbet, K. A. Morris, and D. W. L. Wang, "Control of hysteretic systems: a state-space approach," in *Learning, Control and Hybrid Systems*, Y. Yamamoto and S. Hara, Eds., New York, 1998, vol. 241 of *Lecture Notes in Control and Information Sciences*, pp. 432–451, Springer.
- [17] R. Venkataraman and P. S. Krishnaprasad, "A model for a thin magnetostrictive actuator," in *Proceedings of the 32nd Conference on Information Sciences and Systems, Princeton, NJ*, Princeton, Mar. 1998.
- [18] R. Venkataraman and P. S. Krishnaprasad, "Approximate inversion of hysteresis: theory and numerical results," in *Proceedings of the 39th IEEE Conference on Decision and Control*, Sydney, Australia, Dec. 2000, pp. 4448–4454.
- [19] M. Brokate and A. Visintin, "Properties of the Preisach model for hysteresis," *Journal für die reine und angewandte Mathematik*, vol. 402, pp. 1–40, 1989.
- [20] H. K. Khalil, *Nonlinear Systems*, Prentice Hall, Upper Saddle River, NJ, 1996.
- [21] X. Tan and J. S. Baras, "Control of smart actuators: A viscosity solutions approach," Tech. Rep. TR2001-39, Institute for Systems Research, University of Maryland at College Park, 2001.